◆ Human Brain Mapping 36:883–896 (2015) ◆

Stimulus Dependence of Contralateral Dominance in Human Auditory Cortex

Alexander Gutschalk* **and Iris Steinmann**

Department of Neurology, Universität Heidelberg, 69120 Heidelberg, Germany

Abstract: The auditory system is often considered to show little contralateral dominance but physiological reports on the contralateral dominance of activity evoked by monaural sound vary widely. Here, we show that part of this variation is stimulus-dependent: blood oxygen level dependent (BOLD) responses to 32 s of monaurally presented unmodulated noise (UN) showed activation in contralateral auditory cortex (AC) and deactivation in ipsilateral AC compared to nonstimulus baseline. Slow amplitude-modulated (AM) noise evoked strong contralateral activation and minimal ipsilateral activation. The contrast of AM–versus-UN was used to separate fMRI activity related to the slow amplitude modulation per se. This difference activation was bilateral although still stronger in contralateral AC. In magnetoencephalography (MEG), the response was dominated by the steady-state activity phase locked to the amplitude modulation. This MEG activity showed no consistent contralateral dominance across listeners. Subcortical BOLD activation was strongly contralateral subsequent to the superior olivary complex (SOC) and showed no significant difference between modulated and UN. An acallosal participant showed similar fMRI activation as the group, ruling transcallosal transmission an unlikely source of ipsilateral enhancement or ipsilateral deactivation. These results suggest that ascending activity subsequent to the SOC is strongly dominant contralateral to the stimulus ear. In contrast, the part of BOLD and MEG activity related to slow amplitude modulation is more bilateral and only observed in AC. Ipsilateral deactivation can potentially bias measures of contralateral BOLD dominance and should be considered in future studies. *Hum Brain Mapp 36:883–896, 2015.*

Key words: amplitude modulation; corpus callosum; fMRI; magnetoencephalography; monaural

INTRODUCTION

It has been traditionally noted in clinical neurology that unilateral lesions of the auditory cortex (AC) are not associated with prominent contralesional deficits, in contrast to unilateral lesions of the visual or somatosensory cortex. This apparent lack of contralateral dominance in the AC is generally explained with bilateral projections in the ascending auditory pathway [Adams, 1979; Ades and Brookhart, 1950]. However, part of the ipsilateral projections are inhibitory, for example, those emanating from the lateral superior olive [Glendenning et al., 1992], and many animal models indicate that spiking activity in response to monaural sound is observed almost exclusively in the contralateral inferior colliculus (IC) [Delgutte et al., 1999; Semple and Kitzes, 1985] and medial geniculate nucleus (MGB) [Samson et al., 2000]. Spiking activity in AC may be more variable but is on average also strongly dominant contralateral to the stimulus ear [Brugge et al., 1969; Goldstein et al., 1968; Higgins et al., 2010; Imig et al., 1990; Reser et al., 2000]. In contrast, auditory EEG and magnetoencephalography (MEG) responses evoked by monaural sound in human AC show only

Additional Supporting Information may be found in the online version of this article.

Contract grant sponsor: Bundesministerium für Bildung und Forschung (BMBF); Contract grant number: 01EV0712 (to A.G.)

*Correspondence to: Alexander Gutschalk, Department of Neurology, Universitätsklinikum Heidelberg, Im Neuenheimer Feld 400, 69120 Heidelberg, Germany. E-mail: Alexander.Gutschalk@med.uni-heidelberg.de

Received for publication 23 June 2014; Revised 13 October 2014; Accepted 15 October 2014.

DOI: 10.1002/hbm.22673

Published online 24 October 2014 in Wiley Online Library (wileyonlinelibrary.com).

relative contralateral dominance with amplitude differences of only 10% to 50% between left and right AC [Hine and Debener, 2007; Königs and Gutschalk, 2012; Pantev et al., 1986; Ross et al., 2005; Scherg and Von Cramon, 1986]. Strong lateralization to the contralateral AC has been found in a number of fMRI studies using monaural stimulus presentation [Langers et al., 2005; Schönwiesner et al., 2007; Woldorff et al., 1999], whereas others also reported considerably strong ipsilateral AC activation [Devlin et al., 2003; Lehmann et al., 2007]. The sources of this variability remain obscure.

The interest in understanding contralateral dominance in AC reaches beyond the phenomenon itself and its role for sound localization [Ahveninen et al., 2014]. For example, the structural model to explain the right-ear advantage in dichotic listening is based on the assumption of (1) predominantly contralateral representation in the AC that is further enhanced by ipsilateral input and (2) left-hemispheric dominance for language [Kimura, 1961; Sparks and Geschwind, 1968]. Despite the time that has passed since the introduction of dichotic paradigms, the key parameters contralateral–versus-ipsilateral representation of monaural sound in the AC and the role of transcallosal communication between the auditory cortices [Westerhausen and Hugdahl, 2008] remain incompletely specified.

Here, we explore stimulus-related explanations for the variability of contralateral dominance for monaural sound in AC and the subcortical auditory pathway. In particular, we aimed to integrate the finding of generally weak contralateral dominance in MEG compared to strong contralateral dominance in a subset of fMRI studies (as well as the animal models referenced earlier).

Auditory evoked MEG responses are either coupled to the onset of or change within a sound. Such transient events are typically repeated within a sequence and the MEG response is averaged across trials. The situation is similar for periodic stimuli, like amplitude-modulated (AM) sound, where the steady-state MEG response is locked to the repetitive modulation cycles. AM stimuli can be decomposed into the carrier signal and the AM. While parts of the fMRI response may be related to the AM itself—similar to the phase-locked MEG response—it may also comprise components that reflect the fine structure of the carrier, irrespective of the presence or absence of AM. This hypothetical blood oxygen level dependent (BOLD) response evoked by the carrier may not necessarily have a strong counterpart in MEG. (Conversely, ongoing sounds evoke sustained fields in MEG that can be partly related to the carrier but which do not have a strong BOLD counterpart [Gutschalk et al., 2010; Steinmann and Gutschalk, 2012]). Based on a separation of carrier- and AM-evoked BOLD activity, the discrepancy in contralateral dominance of MEG and BOLD responses in the AC could be resolved under the hypothesis that (I) the AM-evoked response shows little contralateral dominance, whereas (II) the carrier evoked BOLD response exhibits strong contralateral dominance.

To separate these components, we used slow AM with a modulation frequency of 8 Hz, which drives the cortex with an ongoing, phase-locked response in MEG [Wang et al., 2012]. AM-specific BOLD activity was then estimated by contrasting the AM stimulus with the unmodulated noise (UN) carrier [Steinmann and Gutschalk, 2011]. We expected that the AM-specific response was bilateral in MEG and fMRI, and that the remaining activity—evoked by the UN carrier—was more strongly lateralized to contralateral AC. Furthermore, we used cardiac gating [Guimaraes et al., 1998] to obtain activity in the auditory brainstem and evaluate if different lateralization patterns emerge in the ascending auditory pathway.

MATERIALS AND METHODS

Subjects

Twelve listeners (six female and six male) participated in the main fMRI study, and 11 of these listeners also participated in the main MEG study. The mean age was 23.9 years with an age range from 19 to 31 years. Two additional listeners participated in supplementary experiments. One listener (40 years, male) participated in an fMRI experiment to evaluate the influence of the scanner coolant pump. Another listener (37 years, female) with incidentally discovered callosal agenesis was studied with MEG and fMRI to evaluate the influence of transcallosal connection for the results of the main study. The study was approved by the ethics committee of Heidelberg University and written informed consent was obtained from all listeners.

Stimuli and Sound Presentation

Stimuli were 32-s-long segments of white noise, low-pass filtered at 8,000 Hz (second order Butterworth filter), and sampled at 48,000 Hz. The noise was either UN or AM noise with a modulation rate of 8 Hz obtained by modulating the noise with a rectified 4-Hz sinusoid. The stimulus presentation was monaural to the left or right ear. The four stimulus conditions (AM left, AM right, UN left, and UN right) were presented in alternation. The silent interval between successive noise intervals was on average around 32 s (range 24–40 s) in fMRI and 5 s in MEG. In fMRI, the stimuli were presented with S14 insert earphones (Sensimetrics Corporation, Malden, MA). In MEG, the stimuli were presented with ER3 transducers (Etymotic Research, Elk Grove Village, IL) connected to foam earpieces via 1-m-long plastic tubes. The sound level was 85 dB SPL in fMRI and 75 dB SPL in MEG. The lower level in MEG was chosen because of the very low ambient noise level, in which 85 dB were subjectively perceived as unpleasantly loud, whereas the same level was still judged as convenient in the fMRI setting. Each of the four stimulus conditions (left and right, AM and UN) was presented 12 times in fMRI and 25 times in MEG. The total duration of

functional data acquisition was approximately 52 min in fMRI and 62 min in MEG.

MRI Data Acquisition

MRI data were obtained with a 3T, Magnetom Tim Trio scanner (Siemens, Erlangen, Germany), equipped with a 32-channel phased-array head coil. Cardiac gating [Guimaraes et al., 1998] was used to reduce signal fluctuations in the brainstem due to pulse-pressure waves of the basilar artery. To this end, peripheral pulse oximetry was continuously recorded at the subjects' index finger and the TR was adjusted to a minimum of 7.5 s. The acquisition was started with the next pulse after the 7.5 s interval, such that the TR was in a range of 7.5–8.5 s for an average pulse rate of 60 beats per minute. The acquisition time was 1.5 s, leaving approximately 6.5-s long pauses in which the stimulus was presented without the scanner noise [Edmister et al., 1999; Hall et al., 1999]. The functional volume was approximately coronal, tilted toward frontal to cover the AC and the brainstem. 22 T2*-weighted slices (Flip Angle 90°; Echo Time 42 ms) were acquired with 2 mm thickness, 0.1 mm distance, and in-plane resolution of 120 × 120. The field of view was 208 × 208 mm, yielding a voxel size of 1.7 × 1.7 × 2 mm. The timing between acquisition and stimulus onset was staggered in steps of 2 s to resample the BOLD activation time courses in approximately 2-s long intervals. To this end, the stimulus presentation was started with a delay of 0, 2, 4, or 6 s to the acquisition directly preceding the stimulus. The order of delays and interstimulus intervals was pseudorandom and each delay was repeated with the same frequency. A whole-head T1 weighted MPRAGE anatomical sequences was acquired with a voxel size of 1 × 1 × 1.3 mm for anatomical coregistration.

MEG Data Acquisition

MEG data were recorded with a Neuromag 122 system (Elekta Neuromag, Helsinki, Finland) inside a four-layer magnetically shielded room (IMEDCO, Hägendorf, Switzerland). Data were acquired continuously with a 1000-Hz sampling rate (recording bandwidths 0–330 Hz). Before recording, the position of four head-position-indicator coils were measured to register the head position inside the MEG dewar. The position of these coils was digitized with an Isotrack II digitizer (Polhemus, Colchester, VT) relative to 35 predefined points at the head surface.

fMRI Data Analysis

The MRI data were analyzed with the Freesurfer software package version 5.2 (Athinoula A. Martinos Center for Biomedical Imaging, Charlestown, MA), following the standard processing stream. The structural whole-head MPRAGE images were averaged, segmented, and the cortical surface was transformed into a two-dimensional (2D) surface reconstruction. The cortical surface reconstruction was then coregistered with a standard brain for normalization across subjects [Fischl et al., 1999]. Activation maps were calculated by a general linear model using a single-gamma (delta = 2.25 s; tau = 1.25 s) hemodynamic response function [Dale and Buckner, 1997]. Because the Freesurfer functional analysis stream (FS-fast) is designed for a fixed TR, the parameter files were adjusted to produce an exact timing of sound onset and offset relative to the acquisition under the assumption of a fixed TR of 8 s. The timing of stimulus onsets were calculated such that the delay relative to the acquisition before stimulus onset was exact. To adjust the timing between sound offset and the subsequent scanner acquisition, the event duration in the paradigm file was modified for each trial. No timing correction was applied for acquisitions between sound onset and offset, but the deviance from the 8-s TR resulting from the cardiac gating was generally so small in these intervals that it could be neglected. The T1 fluctuation introduced by the variable TR is so small for the long TR > 7.5 s that it can be neglected; accordingly, we did not use interpolation of T1 values to a constant TR [Guimaraes et al., 1998]. The group analysis used a weighted least squares random-effects analysis performed in volume space for subcortical activity and in surface space for cortical activity. To correct for multiple comparisons, the activated voxels (determined by a voxel-wise uncorrected significance threshold of $P < 0.05$) were clustered and significance levels of the clusters were estimated by Monte-Carlo simulation of z-statistics [Hagler et al., 2006]. A threshold of $P < 0.05$ was used for cluster-wise thresholding in this process. Two main contrasts were calculated for each ear: (1) sound (AM + UN)-versus-silence and (2) AM noise-versus-UN. We also evaluated the single AM and UN–versus-silence contrasts at the cortical level, because the two conditions were significantly different here.

A region of interest (ROI) analysis was performed to quantify activity in anatomically defined areas specified in average volume space. AC was defined as the transverse gyri of Heschl, the planum temporale, and the superior temporal gyrus posterior to its intersection with the first transverse gyrus. Subcortical nuclei were determined based on macroscopic anatomy of the average brain in combination with a detailed atlas of brainstem nuclei [Paxinos et al., 2012] and with cross reference to the activation maps obtained for the sound-versus-silence contrast. One sphere for each side was used with the following Talairach center coordinates: (1) cochlear nucleus (CN): ±12, $y = -41.5$, $z = -34$, diameter 6 mm. (2) Superior olivary complex (SOC): $x = \pm 6$, $y = -38$, $z = -32$, diameter 6 mm. (3) Nuclei of the lateral lemniscus (NLL): $x = \pm 10$, $y = -35$, $z = -17$, diameter 6 mm. (4) IC: $x = \pm 5$, $y = -35$, $z = -7$, diameter 6 mm. (5) medial geniculate body (MGB): $x = \pm 16$, $y = -26$, $z = -3$, diameter 7 mm. Only voxels that were active in the sound-versus-silence contrast and that lay within the anatomically specified region were used for analysis. The contralateral stimulus was used for the

definition of all ROIs from SOC to AC. Only the CN ROI was defined based on the ipsilateral stimulus condition. (The contralateral/ipsilateral sound-versus-silence contrast rather than an all sound-versus-silence contrast was used for ROI definition, because the activation pattern for left- and right-ear stimulation were so opposite to each other that a combination of the two decreased the signal-to-noise ratio). The same set of voxels was then used to estimate activity in the respective anatomical area for all four stimulus conditions based on the beta values estimated in the first-level analysis for each subject.

BOLD time courses were reconstructed from the cortical data to separately estimate the contribution of transient and sustained BOLD components. To extract BOLD time courses in the AC ROI, the acquisitions were resorted relative to tone onset and binned to a temporal resolution of 2 s (i.e., 0.5 Hz). The time courses were low-pass filtered at 0.1 Hz (second order, Butterworth filter with zero-phase shift) and averaged across voxels within the AC ROI and then across subjects with MATLAB. A baseline was calculated in the time interval 8 s before sound onset and subtracted from the whole waveform. BOLD amplitudes were measured in the reconstructed waveforms. Peak amplitudes of the transient onset response were measured in the time interval 2–14 s and average amplitudes of the sustained BOLD response were measured in the time interval 14–34 s after sound onset. The data were statistically evaluated with an ANOVA for repeated measures with the factors ear of stimulation (left or right), hemisphere (left or right), and stimulus condition (UM or AM) using SAS version 9.2 (SAS Institute, Cary).

MEG Data Analysis

The MEG data were evaluated with BESA version 5.1.6 (BESA GmbH, Gräfelfing, Germany). The focus was on the time-locked steady-state response (SSR) evoked by the 8-Hz amplitude modulation. First, the response was averaged across all cycles of the 32-s long stimuli, leaving a periodic response that represents a mixture of response components. To compare the amplitude in the left and right AC, two dipoles (one in the left and one in the right AC) were fitted: first, a starting solution was fitted to a grand-average of left- and right-ear stimuli. Thereafter, to further improve the dipole fits, the left-sided dipole was fitted again to the right-ear condition leaving the position of the right-sided dipole fixed and vice versa; the fit was performed for the whole 125-ms long period of the SSR. The procedure was repeated until the dipole positions did not change further. This procedure was implemented because the dipole localization for the grand average was less accurate with respect to the anatomical location of AC in a number of subjects. An alternative analysis based on the initial estimate fitted to the grand average produced highly similar source-waveform results. Therefore, a potential bias of this procedure toward contralateral activity can be excluded. The dipoles were then used to derive the source waveforms for the left- and right-ear stimulation separately for each listener. To model external artifacts generated by passing streetcars in a distance of 500 m, the artifacts were identified in the raw data and a principal component analysis (PCA) was calculated for these intervals. The 1–4 PCA components explaining the artifact were retained and added to the dipole model to model the artifacts and avoid projection of the artifacts on the dipole sources [Ille et al., 2002]. The data were low-pass filtered with a cutoff frequency of 150 Hz (6 dB, zero phase shift Butterworth filter).

Response amplitudes in the source waveforms were determined as the root-mean square of the 125-ms cycle. Statistical analysis was performed with an ANOVA for repeated measures with the factors ear of stimulation (left and right) and hemisphere (left and right).

For spectral analysis of auditory-cortex activity, eye movement artifacts were additionally modeled along with the dipoles and the external artifacts (eye movements are not a problem for SSR analysis, because they are temporally not correlated and are suppressed by averaging high numbers of trials). To this end, two regional sources at the position of the eyes were additionally included in the spatial filter to model eye movement artifact. The spatial filter was applied to the continuous MEG data to provide dipole source waveforms focused on the left and right AC. These AC dipole waveforms were then subjected to FFT analysis using 4,000-ms long epochs in MATLAB. For the four stimulus conditions, eight epochs were used to cover each 32-s long stimulus epoch while keeping the phase of the SSR aligned across all epochs. To estimate the baseline spectrum, the epoch was placed 1,000 ms after sound offset until the beginning of the next sound. Two analyses were performed: to analyze the spectral composition of the SSR, the complex FFTs were averaged across all epochs and then spectra were subsequently derived by calculating absolute values. The SSR was then evaluated at the repetition rate of 8 Hz and at harmonic frequencies. To explore other ongoing induced and evoked activity during the 32-s long stimuli, the spectra of each epoch were averaged disregarding phase information. The spectra were separately averaged for all four stimulus conditions and the silent baseline, which was subsequently subtracted from all stimulus conditions. For statistical analysis, the spectra were evaluated in six frequency bands, roughly coinciding with the delta band (1–4 Hz), theta band (4–8 Hz), alpha band (8–12Hz), beta band (12–25 Hz), gamma band (25–80 Hz), and high-gamma band (80–250 Hz). The statistical analysis was performed with an ANOVA for repeated measures with the factors band, ear of stimulation (left and right) and hemisphere (left and right) as well as separately for each frequency band.

Hemispheric lateralization in MEG and fMRI data were additionally evaluated as lateralization index LI defined as $LI = (R - L)/(|R| + |L|)$, where R and L are the amplitudes in the right and left hemisphere, respectively. This

index ranges from −1 for completely left lateralized to +1 for completely right lateralized. For convenient summary, left- and right-ear conditions were summarized such that amplitudes in the contralateral and ipsilateral ear were added before calculation of the index. The sign of the summarized lateralization indices are provided such that positive values indicate that amplitudes are stronger on the contralateral side and negative values indicate that amplitudes are stronger on the ipsilateral side.

RESULTS

Brainstem fMRI Activity

The subcortical analysis of the fMRI data revealed lateralized activation along the auditory pathway in the sound-versus-silence contrast, which was mirrored for left- and right-ear stimulation (Fig. 1). In contrast, no significant activity was found for the AM-versus-UN contrast, which would have separated subcortical AM-specific activity. In the maps, the sound-evoked activity was ipsilateral to the stimulus ear in CN, bilateral in the SOC, and contralateral at subsequent stages, in particular in the IC and the medial geniculate nucleus (MGB). Consistent and mirrored contralateral activity was also observed between the SOC and IC. With reference to a detailed atlas of the human brainstem [Paxinos et al., 2012], this activity is likely generated in the nuclei of the NLL and in the nucleus of the central auditory tract. An exact separation of these nuclei is probably beyond the capability of the method.

The strong lateralization pattern was confirmed by the ROI analysis, which also includes subthreshold activity in the ipsilateral pathway. The average amplitudes for all stages are shown in the lower panels of Figure 1. Activity was predominantly contralateral to the stimulus ear, as is indicated by the ear × hemisphere interaction, in the MGB ($F_{1,11} = 21.28$, $P = 0.0007$), IC ($F_{1,11} = 23.31$, $P = 0.0005$), and NLL ($F_{1,11} = 31.72$, $P = 0.0002$). No significant ear × hemisphere lateralization was observed for the SOC ($F_{1,11} = 1.37$, $P = 0.2659$), where activity was generally bilateral. Activity in the CN was stronger ipsilaterally (ear × hemisphere: $F_{1,11} = 9.00$, $P = 0.0121$), but there was some contralateral activity in this ROI as well. Note, however, that the CN and SOC are close-by in the brainstem such that a complete separation of the two is probably beyond the limitation of the method used here. In accordance with the primary mapping analysis, no significant condition effects or interactions with the factor condition were observed in any of the ROIs.

The ROIs used for this analysis were based on the contralateral sound-versus-baseline contrast (ipsilateral for CN). Since this contrast may potentially bias the results toward contralateral (ipislateral) dominance, we performed the analysis again with an all-sound-versus-baseline contrast, where left- and right-ear stimuli were combined. The results confirmed the analysis for SOC (bilateral) and IC (strong contralateral dominance). In CN, NLL, and MGB, where the signal-to-noise ratio was not so good, the pattern was more noisy but none of the results were contradictory to the data presented above (see Supporting Information Fig. S1).

FMRI Activity in AC

In AC, AM and UN also evoked BOLD activity that was strongly lateralized toward contralateral of the stimulus ear, but the pattern was overall more complex (Fig. 2). First, there was additional deactivation for the sound-versus-baseline contrast in lateral Heschl's gyrus, ipsilateral to the stimulus ear. Separate analysis of the AM and UN conditions showed that deactivation was in particular a characteristic of the UN stimulus (Fig. 2b), whereas the AM-versus-UN contrast showed no deactivation but small spots of ipsilateral activation in AC. Second, the AM-versus-UN contrast revealed significant difference activity in Heschl's gyrus and planum temporale. This difference activity was more bilateral than the sound-versus-silence contrasts, confirming the main hypothesis for the study.

The ROI analysis (Fig. 3a) confirms the overall stronger AC activity for AM-versus-UN ($F_{1,11} = 78.29$, $P < 0.0001$) and shows a similar ear × hemisphere interaction as observed in centers before AC ($F_{1,11} = 74.74$, $P < 0.0001$). Despite prominent ipsilateral activity, the difference between AM and UN is still stronger in the AC contralateral to the stimulation ear (ear × hemisphere × condition: $F_{1,11} = 64.55$, $P < 0.0001$). The stronger contralateral dominance of the AM and UN conditions are also reflected in the lateralization indices, which were 0.85 ± 0.04 (mean ± standard error) for AM and 0.86 ± 0.07 for UN, respectively, compared to only 0.44 ± 0.05 for the AM-specific activity reflected by the AM-versus-UN contrast (difference compared to AM: $S = 39$, $P = 0.0005$; difference compared to UN: $S = 37$, $P = 0.0015$; Wilcoxon signed-rank test). The results of the ROI analysis were confirmed when the all-sound-versus-baseline contrast was used for ROI definition instead (see Supporting Information Fig. S2).

Because a previous report suggests that sustained BOLD components were more strongly lateralized [Lehmann et al., 2007] than the onset transient, we reconstructed cortical BOLD time courses to separately measure transient and sustained contributions (Fig. 3b) [Harms et al., 2005; Harms and Melcher, 2002]. The results indeed showed that there was ipsilateral transient activation for the AM- as well as the UN-versus-baseline contrast, whereas there was only little evidence of transient BOLD activity in the AM-versus-UN subtraction. Amplitudes measured at the maximum of the transient and in the purely sustained part of the BOLD response are shown in panels c and d of Figure 3. The statistical analysis confirmed most of the results of the beta-value-based ROI analysis (ear × hemisphere, sustained: $F_{1,11} = 49.95$, $P < 0.0001$, transient: ear × hemisphere: $F_{1,11} = 70.96$, $P < 0.0001$; condition, sustained:

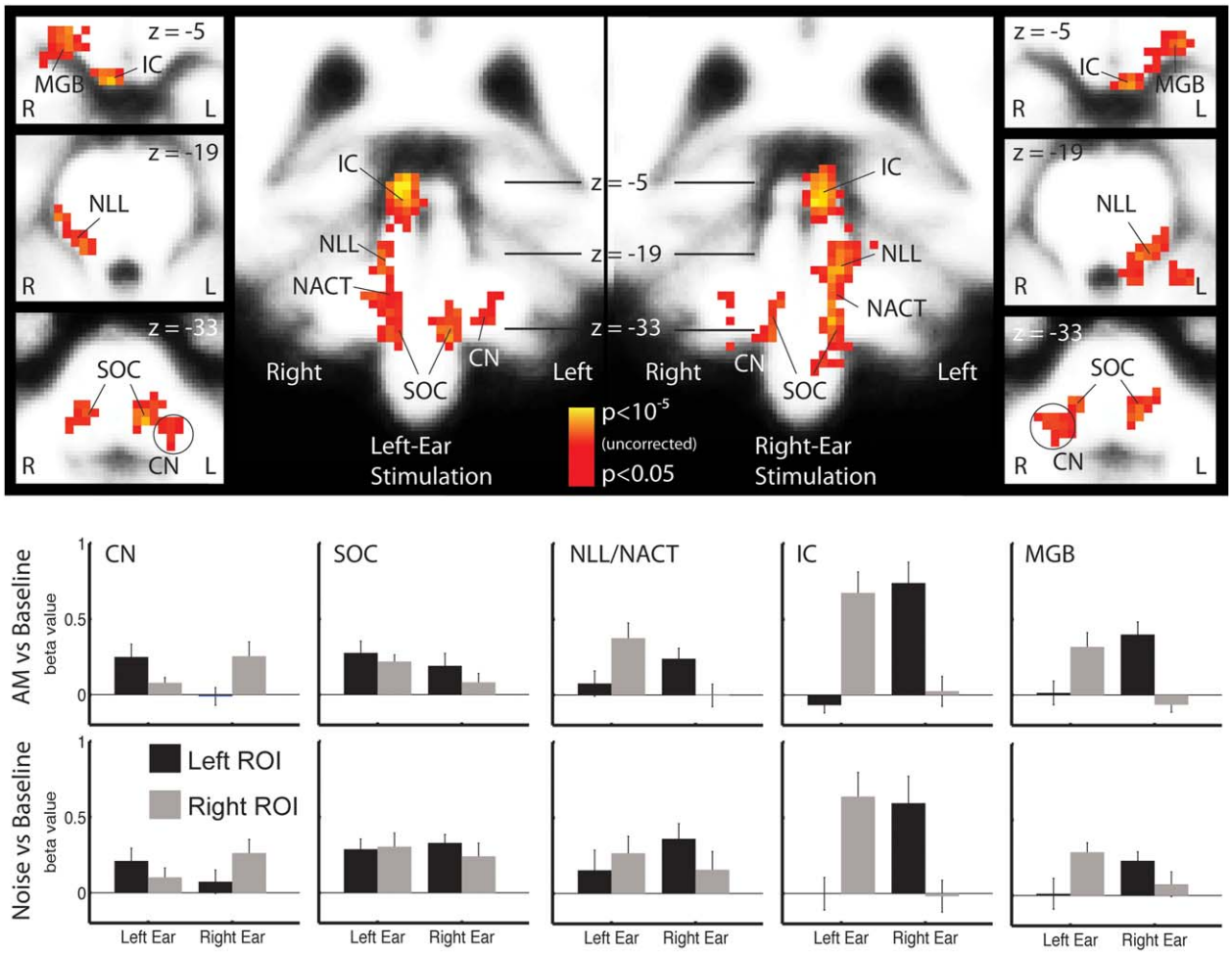

Figure 1.

Brainstem activity maps and ROI analysis. The maps in the upper half of the figure show the sound-versus-silence contrast in the group analysis separately for left- and right-ear stimulation in the left and right half of the figure. The group analysis is corrected for multiple comparisons at the cluster level. Note that the scaling on the voxel level is not corrected for multiple comparison. The ROI analysis shown in the lower half of the figure shows the average activity across listeners (mean ± standard error) for the regions defined in the average brain and using only voxels active in the group analysis. The activation pattern was very similar for UN-versus-baseline (lower panels) and AM noise-versus-baseline (upper panels). There was no significant difference in subcortical nuclei between AM and UN in the ROI analysis or in the voxel-wise group analysis (not shown).

$F_{1,11} = 14.50$, $P = 0.0029$, transient: $F_{1,11} = 8.82$, $P = 0.0128$). However, the ear × hemisphere × condition interaction was only significant for the sustained BOLD (ear × cond × hemisphere $F_{1,11} = 7.86$, $P = 0.0172$), but not for the transient onset component (ear × cond × hemisphere $F_{1,11} = 2.26$, $P < 0.1612$).

The lateralization indices for the sustained BOLD were 0.76 ± 0.06 for AM, 0.74 ± 0.1 for UN, and 0.32 ± 0.12 for AM-versus-UN. Note that the lateralization index for the sustained AM-versus-UN contrast was significantly stronger for left- (LI = 0.37 ± 0.12) compared to right-ear (LI = -0.09 ± 0.08) stimulation ($S = 28$, $P = 0.0269$; Wilcoxon signed-rank test), whereas all other conditions showed no significant differences between left- and right-ear stimulation. One previous fMRI study reported similar asymmetry between left- and right-ear stimulation [Schönwiesner et al., 2007].

The lateralization indices for the onset transients of the BOLD response were 0.51 ± 0.07 for AM and 0.57 ± 0.08 for UN. The transient and sustained BOLD components likely overlap and the measure of the onset transient, therefore, includes some sustained activity. When the lateralization indices are calculated based the difference between onset peak and sustained BOLD amplitude

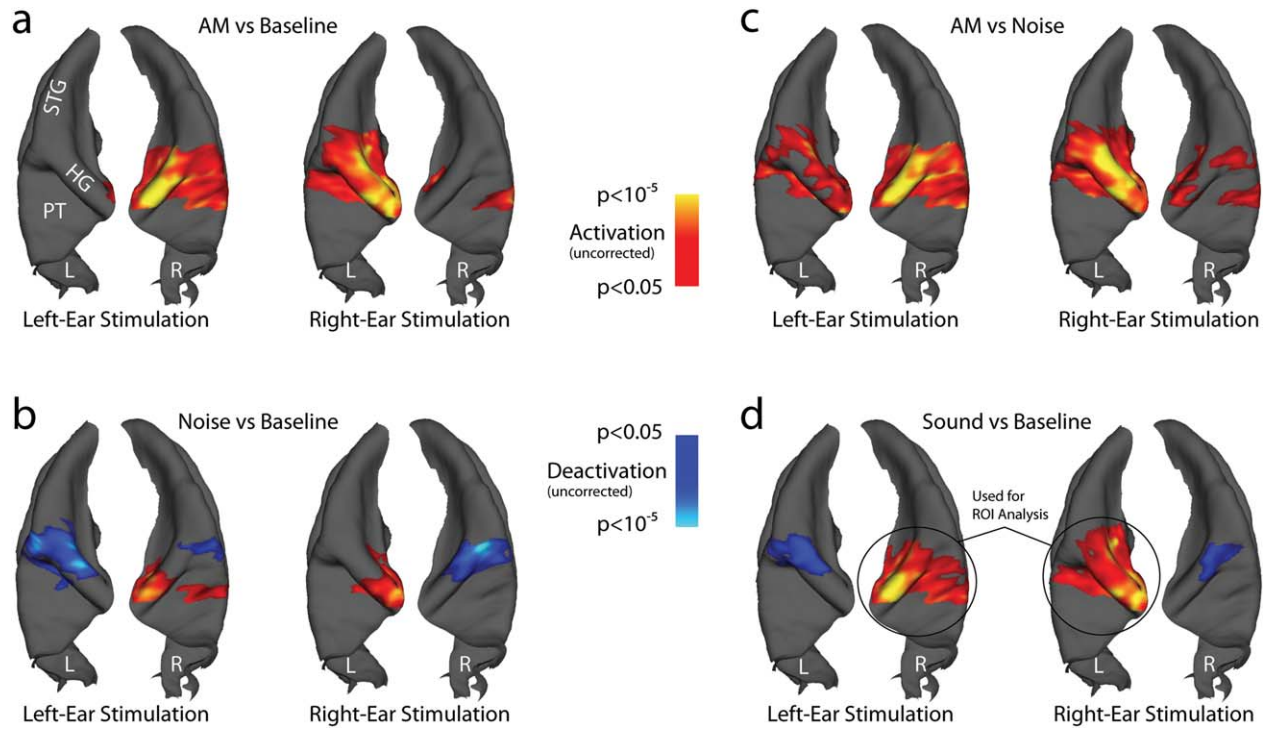

Figure 2.

Group activation maps in the AC. Significant clusters ($P < 0.05$, corrected for multiple comparison at the cluster level) are mapped on a 3D reconstruction of the superior temporal plane (STP) of an average brain, viewed from top. The left (L) and right (R) STP are plotted next to each other for each condition. Main structures seen in this view are Heschl's gyrus (HG), the superior temporal gyrus (STG), and planum temporale (PT). The color coding displays *P* values at the voxel (vertex) level that are not corrected for multiple comparison, with warm colors coding for activation and cold colors coding for deactivation. Four different contrasts are separately shown for left- and right-ear stimulation, to demonstrate the overall symmetry of the results: (**a**) AM noise-versus-baseline contrast. (**b**) UN-versus-baseline contrast. (**c**) AM noise-versus-UN contrast. (**d**) Sound (=AM noise plus UN)-versus-baseline contrast. Like in the subcortical ROI analysis, the contralateral activity of the sound-versus-silence contrast (indicated with black circles) was used for the ROI analysis shown in Figure 3.

instead, their average values are even lower and amount to 0.17 ± 0.06 for AM and 0.08 ± 0.10 for UN, which is in the same range as in the study by Lehmann et al. [2007].

MEG Activity in AC

In MEG, the 8-Hz AM evoked an ongoing SSR. Dipoles fitted to the response projected on average to the intermediate aspect of Heschl's gyrus in the left and right AC (Approximated Talairach coordinates, mean ± standard error, left: $x = -51 \pm 2$, $y = -24 \pm 2$, $z = 8 \pm 2$ right: $x = 49 \pm 2$, $y = -16 \pm 1$, $z = 5 \pm 2$). When the source waveforms were averaged across all cycles, the peaks P_am, P_1m, and N_1m could be identified in the grand average and in most individual listeners (Fig. 4a). The response was generally bilateral and on average stronger in right AC (hemisphere: $F_{1,10} = 7.27$, $P = 0.0225$), as expected based on the structural asymmetry of human AC [Shaw et al., 2013]. However, there was no significant dependence on lateralization on the stimulus ear (ear × hemisphere: $F_{1,10} = 0.17$, $P = 0.6867$). The average lateralization index based on the RMS amplitudes was 0.23 ± 0.10 for left- and 0.12 ± 0.09 for right-ear stimulation, reflecting the general lateralization toward the right AC. The combined lateralization index, which is a better estimate of the stimulus-ear dependence, was on average only 0.04 ± 0.06. Note, however, that some subjects showed convincing contralateral dominance, but two subjects also showed dominance in ipsilateral AC, and that the individual combined lateralization indices ranged from 0.29 (contralateral) to −0.41 (ipsilateral).

An alternative view on the SSR is provided by the FFT analysis shown in Figure 4d. SSRs produce distinct spectral peaks at the repetition rate and its harmonic frequencies, and in the present case five peaks were clearly visible in the average spectrum. The statistical analysis confirmed the on average stronger amplitudes in right AC

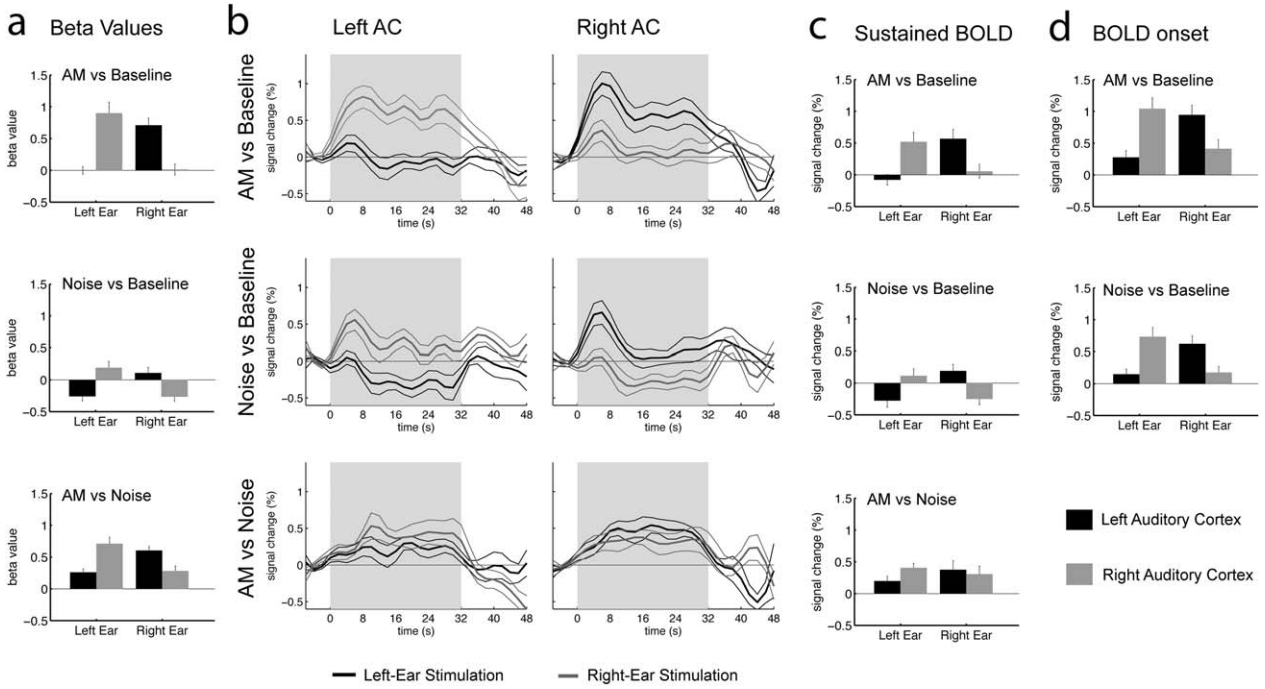

Figure 3.

ROI analysis of BOLD activity in AC. The analysis is based on the contralateral activity in the sound-versus-baseline contrast (Fig. 2d). All graphs show the mean and standard errors across subjects ($N = 12$). Activity in the left AC is plotted in black, activity in the right AC is plotted in gray. The first line in all columns shows the data for the AM-versus-Baseline contrast, the second line the Noise-versus-Baseline contrast, and the third line the AM-versus-Noise contrast. (**a**) Activity estimated by the regression model used to generate the maps in Figure 2. This analysis is equivalent to the subcortical ROI analysis in Figure 1. (**b**) Reconstructed BOLD waveforms for all conditions for the left and right AC ROI. Activity for left-ear stimulation is plotted in black, activity for right-ear stimulation is plotted in gray. These time courses were used to selectively measure (**c**) average sustained BOLD amplitudes in the time range 14–34 s after sound onset, as well as (**d**) peak amplitudes for the onset transient in the time range 2–14 s after sound onset.

(hemisphere: $F_{1,10} = 7.37$, $P = 0.0218$) and the lack of an ear $\times$ hemisphere interaction ($F_{1,10} = 0.11$, $P = 0.7431$). However, there was a trend for an harmonic $\times$ ear $\times$ hemisphere interaction ($F_{4,40} = 3.21$, $P < 0.0807$), the source of which is a differential lateralization of the lower (1–2) and higher (3–5) harmonics of the SSR. While there was a trend for stronger amplitudes in contralateral AC at 8 and 16 Hz ($F_{1,10} = 2.56$, $P = 0.1405$), stronger ipsilateral activity was observed from 24 to 40 Hz ($F_{1,10} = 12.26$, $P = 0.0057$). The summary lateralization indices per frequency band were 0.10 ± 0.09 (8 Hz), 0.17 ± 0.07 (16 Hz), -0.23 ± 0.05 (24 Hz), -0.07 ± 0.08 (32 Hz), and -0.05 ± 0.07 (40 Hz).

Comparison between the individual lateralization indices of the SSR and fMRI activity showed only weak and nonsignificant correlation between lateralization of the 8 Hz component and the AM-versus-UN contrast ($R = 0.58$, $P = 0.0617$), and clearly no significant correlation for the other harmonics.

We also evaluated averaged spectra that disregard phase information to explore if ongoing evoked or induced MEG activity beyond the SSR for AM and UN showed potentially stronger lateralization, or if there was any evidence of lateralized modulation in the alpha or beta bands that could potentially be related to lateralized fMRI activation or deactivation in AC. The analysis revealed enhanced delta- ($F_{1,10} = 15.96$, $P = 0.0025$) and theta-band activity ($F_{1,10} = 12.74$, $P = 0.0051$) for sound-versus-silence contrasts in the AC but no significant enhancement or reduction in the other frequency bands (alpha: $F_{1,10} = 1.31$, $P = 0.2795$; beta: $F_{1,10} = 1.04$, $P = 0.3319$; gamma: $F_{1,10} = 2.54$, $P = 0.1422$; high gamma: $F_{1,10} = 2.65$, $P = 0.1345$). More importantly for the comparison of lateralization in MEG and fMRI, no significant ear $\times$ hemisphere interaction was observed (delta: $F_{1,10} = 0.28$, $P = 0.6052$; theta: $F_{1,10} = 0.39$, $P = 0.5483$; alpha: ear $\times$ hemisphere: $F_{1,10} = 1.09$, $P = 0.3203$; beta: $F_{1,10} = 1.24$, $P = 0.2910$; gamma: $F_{1,10} = 1.31$, $P = 0.2793$; high-Gamma: $F_{1,10} = 3.51$, $P = 0.0905$), nor any other meaningful main effect or interaction. Note that this analysis included the onset and offset transients, but alternative analyses excluding these epochs produced very similar results, suggesting

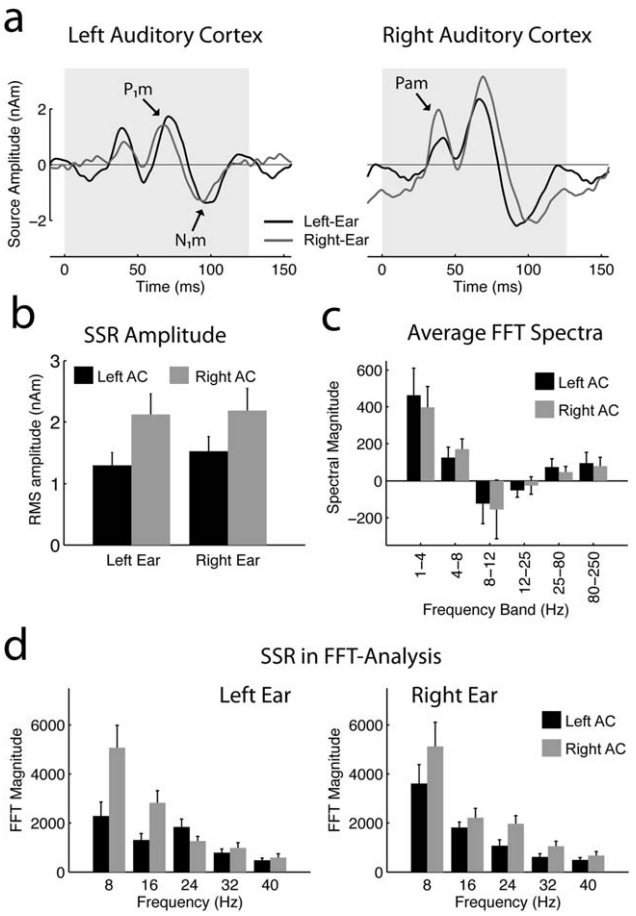

Figure 4.

Summary of MEG data. (**a**) Auditory SSR evoked by the 8-Hz AM in the left and right AC. The data were averaged across all cycles of the 32-s long stimuli. The peaks P_am, P_1m, and N_1m are observed in both hemispheres. (**b**) RMS amplitudes (mean ± standard error; $N = 11$) of the steady-state source waveforms. (**c**) FFT spectra averaged disregarding phase information after subtraction of the baseline activity obtained in silent epochs. The panel shows the sum of all four stimulus conditions (AM and UM, left and right ear), because no significant differences were found between these conditions. No significant ear-dependent lateralization was observed in particular. (**d**) FFT analysis of the SSR for the F0 (8 Hz) and four harmonics at 16, 24, 32, and 40 Hz. The left panel shows the result for left-ear and the right panel for right-ear stimulation. Activity in the left AC is plotted in black, activity in the right AC is plotted in gray.

that it reflects ongoing activity. Finally, we evaluated the evoked sustained fields, a DC component evoked by the ongoing sounds. The sustained fields were evoked bilaterally by the monaural sounds and did not show higher contralateral dominance across subjects. The sustained field was numerically stronger for AM than UN stimuli. At the end of the 32-s stimulus, the sustained field evoked by UN was absent or so small that it could not be reliably detected.

Role of Transcallosal Connections

The finding that activity is enhanced for AM-versus-UN in AC but not in the preceding subcortical centers suggests that the enhancement is related to AC specific processes. Moreover, the strong contralateral activation from NLL up to MGB raises the question whether ipsilateral AC activity evoked by AM requires the transcallosal pathway. Since deactivation was not observed in the subcortical pathway, we also wanted to evaluate if the ipsilateral deactivation in AC is driven by transcallosal projections.

To this end, a listener with callosal agenesis was studied (Fig. 5a) to probe the role of transcallosal connection between the left and right AC. This listener did not show any known neurological or cognitive abnormalities and had been discovered accidentally in an imaging study recruiting normal volunteers; dichotic listening studies established in our laboratory for the workup of central hearing disorders [Gutschalk et al., 2012] revealed normal results.

The fMRI results (Fig. 5b,c) were close to the average and well within the range of the group results shown in Figures 2 and 3. First, ipsilateral activity was relatively stronger in the AM-versus-UN contrast compared to the sound-versus-silence contrasts. Lateralization indices based on beta values (sustained BOLD amplitudes) were 0.92 (0.72) for AM, 1.0 (1.0) for UN, and 0.40 (0.24) for AM-versus-UN. Second, ipsilateral deactivation was on the strong side in the acallosal subject, ruling it unlikely that ipsilateral BOLD deactivation in AC is mediated by transcallosal fibers.

In MEG (Fig. 5d), the 8-Hz steady–steady response showed stronger contralateral dominance than the group average, showing a lateralization index of 0.54 for the 8-Hz harmonic and of 0.28 for the RMS amplitude. Given the previously mentioned broad range of MEG lateralization, however, it cannot be concluded that this stronger contralateral dominance lies outside of the range of the normal population. Moreover, there is still considerable ipsilateral activity in these MEG results and the lateralization is weaker than the lateralization in the sound-versus-silence contrasts in fMRI.

Influence of Scanner Coolant Pump

The fMRI results reported so far were performed with the scanner coolant pump switched on, because routinely switching off the pump for auditory studies is not permitted at our site. However, to exclude a bias of pump sounds on the lateralization results in fMRI, a single subject could be studied with the pump switched off and was then again studied with the pump switched on (see also Supporting Information Fig. S3). There was almost no ipsilateral deactivation in this listener, but this effect was independent of the pump sounds, and if anything deactivation was stronger when the pump was switched off. More importantly, BOLD activity was strongly

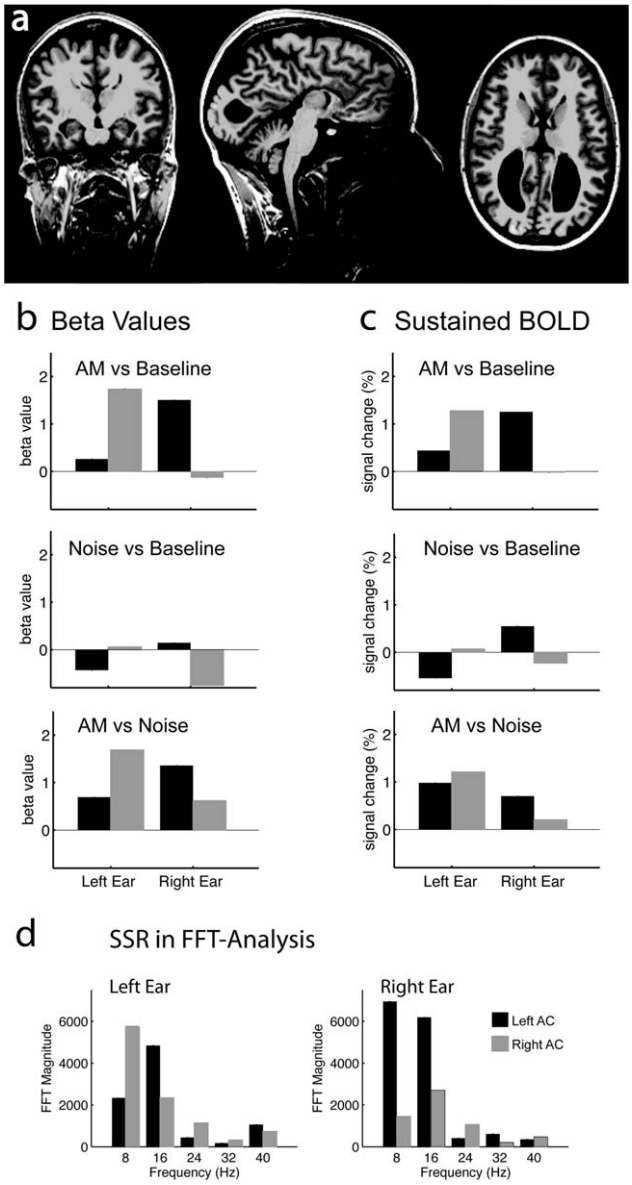

Figure 5.

fMRI and MEG results in an acallosal listener. (**a**) Structural MRI: The complete lack of corpus callosum is accompanied by the typical configuration of the lateral ventricles, but is not associated with any other anomaly. (**b**,**c**) Individual ROI analysis based on activated voxels in the sound-versus-silence contrast. The values in (b) are based on the beta values of the regression analysis (compare with Fig. 3a) and the values in (c) are based on the sustained amplitudes in the reconstructed BOLD time courses (compare with Fig. 3c). (**d**) Individual FFT analysis of the SSR for the left (left panel) and right (right panel) AC (compare with Fig. 4d).

contralateral in the noise-versus-silence condition, whereas the AM-versus-UN contrast was clearly bilateral. In fact, activity in this contrast was somewhat stronger in ipsilateral AC, confirming that the difference in lateralization cannot be attributed to interference with coolant-pump sounds.

DISCUSSION

These results reveal a striking dissociation of hemispheric lateralization in the auditory pathway. While BOLD activity for sound-versus-silence contrasts is strongly lateralized toward the contralateral hemisphere subsequent to the SOC and up to the AC, AM related activity in the AC comprises a considerable share of ipsilateral activity. Our hypothesis was that the AM-versus-UN contrast would best estimate activity related to AM phase locking and, thus, be as bilateral as the phase locked MEG response. The results are generally compatible with this hypothesis but lateralization of the MEG response was still less prominent with lateralization indices of only 0.1–0.2 compared to 0.3–0.4 for the BOLD contrast. Across subjects, the variance of lateralization indices was much larger for MEG than fMRI. One reason for the larger MEG variance is probably signal cancelation that depends on cortical folding and orientation and is, therefore, as variable as individual anatomy [Ahlfors et al., 2010]. In contrast, fMRI is summed irrespective of cortical orientation, limiting the potential for higher individual correlation between BOLD and MEG lateralization. Moreover, the FFT analysis of the MEG data suggests that the 8- and 16-Hz harmonics show a trend for contralateral dominance, whereas the 24-Hz component shows ipsilateral dominance. While these effects are relatively small, their coexistence could be another source of variance in MEG and also explain why the summed MEG activity was dominant in ipsilateral AC in a few subjects.

Lateralization in AC in previous monaural fMRI studies spans from strongly contralateral [Langers et al., 2005; Scheffler et al., 1998], 50% or less contralateral [Behne et al., 2005; Jäncke et al., 2002; Langers et al., 2007; Lehmann et al., 2007; Suzuki et al., 2002; Woldorff et al., 1999] up to not significantly contralateral [Devlin et al., 2003]. Many of these studies used some kind of slow modulation and some used stimulus blocks that are shorter than the ones in this study (typically less than 10 s). Therefore, the individual lateralization might be explained by a blending of three components: First, the strongly lateralized sustained BOLD activity observed for sound-versus-silence contrasts, which is supposedly related to the fine structure of the carrier signal. Second, the weakly lateralized transient onset response [Lehmann et al., 2007]. Third, the weakly lateralized sustained response to slow (AM) fluctuations. Prominent differences in lateralization are accordingly expected in dependence on temporal stimulus characteristics, in particular temporal modulation and sound duration.

There are only few fMRI studies of subcortical activation with monaural stimulation, all of which found strong contralateral but varying degrees of ipsilateral activity in IC

and MGB [Langers et al., 2005; Melcher et al., 2000; Schönwiesner et al., 2007; Boyen et al., 2014]. In the present study, there was strong contralateral activity and no significant ipsilateral activity in IC and MGB across listeners. This finding in the fMRI data may in fact be well in line with single unit studies in the IC of cat [Delgutte et al., 1999; Semple and Aitkin, 1979] and gerbil [Semple and Kitzes, 1985]. Based on these data, almost all IC neurons respond to contralateral sounds, whereas only 20% also respond to ipsilateral sounds and the response for ipsilateral stimulation is typically much weaker than for contralateral stimulation in these neurons [Semple and Kitzes, 1985].

Based on the available data of monaural ipsi- and contralateral stimulation, it appears that spiking activity of single units is still predominantly contralateral in cat MGB [Samson et al., 2000] and primary AC [Brugge et al., 1969; Hall and Goldstein, 1968; Samson et al., 1993]. Analysis of laminar recordings in monkey A1 revealed a dissociation between the thalamorecipient lamina III and supragranular layers for monaural stimulation [Reser et al., 2000]. Predominantly excitatory responses to contralateral- and inhibitory responses to ipsilateral-ear stimulation were observed for early multiunit activity and evoked responses in layer III. However, evoked responses in supragranular layers often showed considerable ipsilateral activity, sometimes associated with longer latency spiking activity.

The bilateral AC activity found in the present study is likely associated with slow stimulus fluctuations. It has been shown that sustained fMRI activity in AC decreases strongly with rates above 20 Hz [Giraud et al., 2000; Harms and Melcher, 2002; Overath et al., 2012] and is then dominated by transient BOLD responses at sound onset and offset, whereas subcortical activity remains sustained at even higher rates [Harms et al., 2005; Harms and Melcher, 2002]. The lack of strong sustained BOLD activity for fast repetition rates is likely related to cortical adaptation, which is similarly found for the long-latency responses in MEG [Hari et al., 1982; Imada et al., 1997]. Assuming that these long-latency responses in the theta range are predominantly generated in supragranular layers of AC [Fishman and Steinschneider, 2012; Lakatos et al., 2013], it is conceivable that slow AM and other slow stimulus fluctuations [Steinmann and Gutschalk, 2012] recruit bilateral processes in supragranular layers that adapt at higher rates and for unmodulated sounds. As link between MEG and BOLD activity, there may either be a direct coupling between BOLD and the slow synaptic activity that generates these MEG responses in the theta range, or alternatively there could be an indirect link, such as for example high-gamma activity that is driven by the theta activity [Lakatos et al., 2005].

Conversely, the strongly contralateral dominant AC activity observed in fMRI is probably more closely linked to the contralateral dominant activity in the subcortical auditory pathway. Potentially this activity is stronger in primary AC, given the finding that UN activation was predominantly located in medial Heschl's gyrus [Hackett et al., 2001]. Notably, the pattern of activated structures for UN is more similar to fMRI activation found for faster AM at 40 Hz, which evokes enhanced sustained activity in IC, MGB, and medial Heschl's gyrus compared to the unmodulated pure tone carrier [Steinmann and Gutschalk, 2011]. This finding matches with the idea that the strongly lateralized activity observed in fMRI is not prone to strong adaptation at faster rates and, therefore, produces strong sustained activity for UN.

The hypothesis that processing in supragranular layers is more bilateral than in the input layers raises the question how the information is then routed to the ipsilateral AC. The results obtained in an acallosal subject presented here make it unlikely that the information is transferred via the corpus callosum and rather suggest that ipsilateral cortical activity is based on enhancement of weaker ipsilateral projections from the MGB. This conclusion is further supported by previous reports of bilateral BOLD activity in AC for monaural stimulation with 20 s of pulsed complex sounds [Paiement et al., 2010] in acallosal listeners. However, conclusions based on acallosal subjects are limited by the presence of alternative interhemispheric connections that develop only in individuals with callosal agenesis but not in normally developing individuals [Paul et al., 2007; Tovar-Moll et al., 2014]. These connections have, for example, been suggested to explain why acallosal subjects—in contrast to callosotomized patients—do not consistently show typical behavioral "split-brain" symptoms such as enhanced right-ear advantage [Lassonde et al., 1990]. Therefore, it cannot yet be excluded with certainty that ipsilateral AC activity observed in our normal listeners was transferred via the corpus callosum, as has been suggested based on animal models [Carrasco et al., 2013], and via alternative pathways in the acallosal listener. Conversely, visual evoked potentials do not show clear ipsilateral activity in acallosal subjects as well as callosotomized patients but do so in subjects with normally developed corpus callosum [Brown et al., 1999]. Therefore, we think that the presence of ipsilateral activity in our acallosal subject in both, MEG and fMRI, indicates that ipsilateral thalamic projections are likely more important for driving ipsilateral activity in AC.

An unexpected but interesting finding of this study is ipsilateral reduction of BOLD activity in comparison to baseline, in particular for UN. Previous studies did not find ipsilateral reduction of BOLD in monaural stimulation to the best of our knowledge, possibly because they mostly used modulated or shorter stimuli. The ipsilateral activation of the onset transient and the response to the modulation may cancel the BOLD deactivation in this case. However, reduction of BOLD activity has been consistently reported in the primary somatosensory cortex ipsilateral to the stimulation [Kastrup et al., 2008; Klingner et al., 2014; Mullinger et al., 2014]. Ipsilateral reduction of BOLD could possibly be a correlate of ipsilateral inhibition observed in binaural compared to monaural conditions [Brugge et al., 1969; Hall and Goldstein, 1968; Samson et al., 1993]. While the latter interpretation would be

intriguing from a physiological perspective, an argument against it could be that deactivation was only found in cortex but not in subcortical stages, where it has been similarly described in single-unit studies [Delgutte et al., 1999; Imig et al., 1990; Samson et al., 2000]. Conversely, it could be that deactivation can only be observed in fMRI in the presence of competing excitation, and that AC simply showed higher activation levels evoked by the baseline noise. An alternative explanation could be related to stimulus-signal fluctuation, because the multisecond noise bursts produce a highly monotonic stimulus with only little signal fluctuation, which could mask more variable sounds in the baseline interval. One such sound source is the scanner coolant pump but no influence of the pump was found in the subject where we tested this possibility. Alternatively, listeners may hear their own breathing and other physiological sound generated in their head more prominently during the baseline interval, whereas these sounds are masked in one ear during stimulation. Because physiological sounds emanating in the head are also heard by bone conduction, they are not much attenuated by passive sound shielding and are hardly controllable in silence. This problem is not limited to the monaural conditions used in the present study but in fact masking of baseline sound should be more efficient with diotic stimulation. However, we did not find deactivation in a previous experiment where we used diotic broadband noise with a similar setup [Steinmann and Gutschalk, 2012], ruling an explanation of deactivation by baseline masking unlikely. Finally, attentional modulation could theoretically be a source of relative reduction of activity. Selective attention in dichotic situations enhances the activity evoked by the attended stream in EEG and MEG [Alho, 1992; Rif et al., 1991], and it has been suggested that this enhancement is somewhat stronger contralateral to the attended ear based on PET and fMRI [Alho et al., 1999; Rinne et al., 2008]. While our stimulus is monaural, other sounds already aforementioned could be considered a stimulus stream in the contralateral ear. If attention is mainly attracted to the stimulus ear, it could be that activity evoked by sounds in the baseline epoch is reduced in the stimulus epoch relative to the baseline epoch (on top of the monaural masking discussed earlier). In this case, the BOLD reduction would be expected to be bilateral and only appear to be ipsilateral because it is canceled in the AC contralateral to the monaural stimulation. An explanation of ipsilateral BOLD reduction based on attention does, therefore, appear rather unlikely but cannot be ruled out completely at this point. Exploring the source of ipsilateral BOLD reduction in more detail appears worthwhile the effort.

It is important to note that ipsilateral deactivation may interfere with measures of contralateral dominance: consider the possibility that sources of BOLD activation and deactivation may coexist and, thus, cancel within the resolution of one voxel. This scenario could provide an alternative explanation for the stronger contralateral dominance of UN-and AM-versus-baseline compared to the AM-versus-UN contrasts, provided the amount of ipsilateral deactivation is relatively similar for AM and UN and does not scale with the amount of activation. It could then be that ipsilateral deactivation dominates the UN-versus-baseline contrast because there is relatively little ipsilateral activation. Deactivation and activation are balanced in ipsilateral AC for the AM-versus-baseline contrast, because ipsilateral activity is stronger but still all ipsilateral activation is swamped by ipsilateral deactivation. In contrast, the ipsilateral response enhancement is revealed by the AM-versus-UN contrast, because the deactivation is of equal strengths for UN and AM and would then be eliminated by subtraction. Moreover, the neural underpinnings of BOLD deactivation may have no influence on the MEG response and could then explain the stronger contralateral dominance in BOLD compared to MEG measures. One reason why we think that the strong contralateral dominance of BOLD activation in AC is real, nevertheless, is the equally strong contralateral dominance that we found in the subcortical auditory pathway, where we found no evidence of deactivation. Since the subcortical activity was not sensitive to the presence of slow AM, it is supposedly more closely related to the stimulus fine structure. The contralateral dominance of the subcortical activity, therefore, supports the interpretation that activity driven by the carrier fine structure shows generally stronger contralateral dominance, whereas cortical activity driven by slow AM and sound onsets is overall more bilateral.

In summary, the present data suggest that AM—or slow stimulus fluctuations in general—recruit processes in AC that operate on the incoming information of the ascending auditory pathway but are specific to cortical processing. These processes are reflected by the enhanced activity for AM-versus-UN in fMRI, and the phase-locked activity in the alpha and theta bands in MEG. AM driven activity is distinct from afferent activity in the ascending pathway with respect to its higher amount of ipsilateral activation. Since the ipsilateral activity is similarly present in the absence of transcallosal fibers, it is likely that the AM induced fMRI and MEG activity enhances input from ipsilateral projections, or that it operates on a subset of afferents that are more bilateral than the gross of activity observed in the subcortical pathway in fMRI, for example, in non-lemniscal pathways [Ayala et al., 2012].

REFERENCES

Adams JC (1979): Acending projections to the inferior colliculus. J Comp Neurol 183:519–538.

Ades HW, Brookhart JM (1950): The central auditory pathway. J Neurophysiol 13:189–205.

Ahlfors SP, Han J, Lin FH, Witzel T, Belliveau JW, Hämäläinen MS, Halgren E (2010): Cancellation of EEG and MEG signals generated by extended and distributed sources. Hum Brain Mapp 31:140–149.

Ahveninen J, Kopco N, Jaaskelainen IP (2014): Psychophysics and neuronal bases of sound localization in humans. Hear Res 307:86–97.

Alho K (1992): Selective attention in auditory processing as reflected by event-related brain potentials. Psychophysiology 29:247–263.

Alho K, Medvedev SV, Pakhomov SV, Roudas MS, Tervaniemi M, Reinikainen K, Zeffiro T, Naatanen R (1999): Selective tuning of the left and right auditory cortices during spatially directed attention. Brain Res Cogn Brain Res 7:335–341.

Ayala YA, Perez-Gonzalez D, Duque D, Nelken I, Malmierca MS (2012): Frequency discrimination and stimulus deviance in the inferior colliculus and cochlear nucleus. Front Neural Circuits 6:119.

Behne N, Scheich H, Brechmann A (2005): Contralateral white noise selectively changes right human auditory cortex activity caused by a FM-direction task. J Neurophysiol 93:414–423.

Boyen K, de Kleine E, van Dijk P, Langers DRM (2014): Tinnitus-related dissociation between cortical and subcortical neural activity in humans with mild to moderate sensorineural hearing loss. Hear Res 312:48–59.

Brown WS, Jeeves MA, Dietrich R, Burnison DS (1999): Bilateral field advantage and evoked potential interhemispheric transmission in commissurotomy and callosal agenesis. Neuropsychologia 37:1165–1180.

Brugge JF, Dubrovsky NA, Aitkin LM, Anderson DJ (1969): Sensitivity of single neurons in auditory cortex of cat to binaural tonal stimulation; effects of varying interaural time and intensity. J Neurophysiol 32:1005–1024.

Carrasco A, Brown TA, Kok MA, Chabot N, Kral A, Lomber SG (2013): Influence of core auditory cortical areas on acoustically evoked activity in contralateral primary auditory cortex. J Neurosci 33:776–789.

Dale AM, Buckner RL (1997): Selective averaging of rapidly presented individual trials using fMRI. Hum Brain Mapp 5:329–340.

Delgutte B, Joris PX, Litovsky RY, Yin TC (1999): Receptive fields and binaural interactions for virtual-space stimuli in the cat inferior colliculus. J Neurophysiol 81:2833–2851.

Devlin JT, Raley J, Tunbridge E, Lanary K, Floyer-Lea A, Narain C, Cohen I, Behrens T, Jezzard P, Matthews PM (2003): Functional asymmetry for auditory processing in human primary auditory cortex. J Neurosci 23:11516–11522.

Edmister WB, Talavage TM, Ledden PJ, Weisskoff RM (1999): Improved auditory cortex imaging using clustered volume acquisitions. Hum Brain Mapp 7:89–97.

Fischl B, Sereno MI, Dale AM (1999): Cortical surface-based analysis. II: Inflation, flattening, and a surface-based coordinate system. Neuroimage 9:195–207.

Fishman YI, Steinschneider M (2012): Searching for the mismatch negativity in primary auditory cortex of the awake monkey: Deviance detection or stimulus specific adaptation? J Neurosci 32:15747–15758.

Giraud AL, Lorenzi C, Ashburner J, Wable J, Johnsrude I, Frackowiak R, Kleinschmidt A (2000): Representation of the temporal envelope of sounds in the human brain. J Neurophysiol 84:1588–1598.

Glendenning KK, Baker BN, Hutson KA, Masterton RB (1992): Acoustic chiasm V: Inhibition and excitation in the ipsilateral and contralateral projections of LSO. J Comp Neurol 319:100–122.

Goldstein MH Jr, Hall JL II, Butterfield BO (1968): Single-unit activity in the primary auditory cortex of unanesthetized cats. J Acoust Soc Am 43:444–455.

Guimaraes AR, Melcher JR, Talavage TM, Baker JR, Ledden P, Rosen BR, Kiang NY, Fullerton BC, Weisskoff RM (1998): Imaging subcortical auditory activity in humans. Hum Brain Mapp 6:33–41.

Gutschalk A, Brandt T, Bartsch A, Jansen C (2012): Comparison of auditory deficits associated with neglect and auditory cortex lesions. Neuropsychologia 50:926–938.

Gutschalk A, Hämäläinen MS, Melcher JR (2010): BOLD responses in human auditory cortex are more closely related to transient MEG responses than to sustained ones. J Neurophysiol 103: 2015–2026.

Hackett TA, Preuss TM, Kaas JH (2001): Architectonic identification of the core region in auditory cortex of macaques, chimpanzees, and humans. J Comp Neurol 441:197–222.

Hagler DJ Jr, Saygin AP, Sereno MI (2006): Smoothing and cluster thresholding for cortical surface-based group analysis of fMRI data. Neuroimage 33:1093–1103.

Hall DA, Haggard MP, Akeroyd MA, Palmer AR, Summerfield AQ, Elliott MR, Gurney EM, Bowtell RW (1999): "Sparse" temporal sampling in auditory fMRI. Hum Brain Mapp 7:213–223.

Hall JL II, Goldstein MH Jr (1968): Representation of binaural stimuli by single units in primary auditory cortex of unanesthetized cats. J Acoust Soc Am 43:456–461.

Hari R, Kaila K, Katila T, Tuomisto T, Varpula T (1982): Interstimulus interval dependence of the auditory vertex response and its magnetic counterpart: Implications for their neural generation. Electroencephalogr Clin Neurophysiol 54:561–569.

Harms MP, Guinan JJ Jr, Sigalovsky IS, Melcher JR (2005): Short-term sound temporal envelope characteristics determine multisecond time patterns of activity in human auditory cortex as shown by fMRI. J Neurophysiol 93:210–222.

Harms MP, Melcher JR (2002): Sound repetition rate in the human auditory pathway: Representations in the waveshape and amplitude of fMRI activation. J Neurophysiol 88:1433–1450.

Higgins NC, Storace DA, Escabi MA, Read HL (2010): Specialization of binaural responses in ventral auditory cortices. J Neurosci 30:14522–14532.

Hine J, Debener S (2007): Late auditory evoked potentials asymmetry revisited. Clin Neurophysiol 118:1274–1285.

Ille N, Berg P, Scherg M (2002): Artifact correction of the ongoing EEG using spatial filters based on artifact and brain signal topographies. J Clin Neurophysiol 19:113–124.

Imada T, Watanabe M, Mashiko T, Kawakatsu M, Kotani M (1997): The silent period between sounds has a stronger effect than the interstimulus interval on auditory evoked magnetic fields. Electroencephalogr Clin Neurophysiol 102:37–45.

Imig TJ, Irons WA, Samson FR (1990): Single-unit selectivity to azimuthal direction and sound pressure level of noise bursts in cat high-frequency primary auditory cortex. J Neurophysiol 63:1448–1466.

Jäncke L, Wüstenberg T, Schulze K, Heinze HJ (2002): Asymmetric hemodynamic responses of the human auditory cortex to monaural and binaural stimulation. Hear Res 170:166–178.

Kastrup A, Baudewig J, Schnaudigel S, Huonker R, Becker L, Sohns JM, Dechent P, Klingner C, Witte OW (2008): Behavioral correlates of negative BOLD signal changes in the primary somatosensory cortex. Neuroimage 41:1364–1371.

Kimura D (1961): Some effects of temporal-lobe damage on auditory perception. Can J Psychol 15:156–165.

Klingner CM, Hasler C, Brodoehl S, Witte OW (2014): Excitatory and inhibitory mechanisms underlying somatosensory habituation. Hum Brain Mapp 35:152–160.

Königs L, Gutschalk A (2012): Functional lateralization in auditory cortex under informational masking and in silence. Eur J Neurosci 36:3283–3290.

Lakatos P, Musacchia G, O'Connel MN, Falchier AY, Javitt DC, Schroeder CE (2013): The spectrotemporal filter mechanism of auditory selective attention. Neuron 77:750–761.

Lakatos P, Shah AS, Knuth KH, Ulbert I, Karmos G, Schroeder CE (2005): An oscillatory hierarchy controlling neuronal excitability and stimulus processing in the auditory cortex. J Neurophysiol 94:1904–1911.

Langers DR, Backes WH, van Dijk P (2007): Representation of lateralization and tonotopy in primary versus secondary human auditory cortex. Neuroimage 34:264–273.

Langers DR, van Dijk P, Backes WH (2005): Lateralization, connectivity and plasticity in the human central auditory system. Neuroimage 28:490–499.

Lassonde M, Bryden MP, Demers P (1990): The corpus callosum and cerebral speech lateralization. Brain Lang 38:195–206.

Lehmann C, Herdener M, Schneider P, Federspiel A, Bach DR, Esposito F, di Salle F, Scheffler K, Kretz R, Dierks T, Seifritz E (2007): Dissociated lateralization of transient and sustained blood oxygen level-dependent signal components in human primary auditory cortex. Neuroimage 34:1637–1642.

Melcher JR, Sigalovsky IS, Guinan JJ Jr, Levine RA (2000): Lateralized tinnitus studied with functional magnetic resonance imaging: Abnormal inferior colliculus activation. J Neurophysiol 83:1058–1072.

Mullinger KJ, Mayhew SD, Bagshaw AP, Bowtell R, Francis ST (2014): Evidence that the negative BOLD response is neuronal in origin: A simultaneous EEG-BOLD-CBF study in humans. Neuroimage 94:263–274.

Overath T, Zhang Y, Sanes DH, Poeppel D (2012): Sensitivity to temporal modulation rate and spectral bandwidth in the human auditory system: fMRI evidence. J Neurophysiol 107:2042–2056.

Paiement P, Champoux F, Bacon BA, Lassonde M, Mensour B, Leroux JM, Lepore F (2010): Functional reorganization of the auditory pathways (or lack thereof) in callosal agenesis is predicted by monaural sound localization performance. Neuropsychologia 48:601–606.

Pantev C, Lütkenhöner B, Hoke M, Lehnertz K (1986): Comparison between simultaneously recorded auditory-evoked magnetic fields and potentials elicited by ipsilateral, contralateral and binaural tone burst stimulation. Audiology 25:54–61.

Paul LK, Brown WS, Adolphs R, Tyszka JM, Richards LJ, Mukherjee P, Sherr EH (2007): Agenesis of the corpus callosum: Genetic, developmental and functional aspects of connectivity. Nat Rev Neurosci 8:287–299.

Paxinos G, Huang X, Sengul G, Watson C (2012): Organization of Brainstem Nuclei. The Human Nervous System. Amsterdam: Elsevier Academic Press. pp 260–327.

Reser DH, Fishman YI, Arezzo JC, Steinschneider M (2000): Binaural interactions in primary auditory cortex of the awake macaque. Cereb Cortex 10:574–584.

Rif J, Hari R, Hämäläinen MS, Sams M (1991): Auditory attention affects two different areas in the human supratemporal cortex. Electroencephalogr Clin Neurophysiol 79:464–472.

Rinne T, Balk MH, Koistinen S, Autti T, Alho K, Sams M (2008): Auditory selective attention modulates activation of human inferior colliculus. J Neurophysiol 100:3323–3327.

Ross B, Herdman AT, Pantev C (2005): Right hemispheric laterality of human 40 Hz auditory steady-state responses. Cereb Cortex 15:2029–2039.

Samson FK, Barone P, Irons WA, Clarey JC, Poirier P, Imig TJ (2000): Directionality derived from differential sensitivity to monaural and binaural cues in the cat's medial geniculate body. J Neurophysiol 84:1330–1345.

Samson FK, Clarey JC, Barone P, Imig TJ (1993): Effects of ear plugging on single-unit azimuth sensitivity in cat primary auditory cortex. I. Evidence for monaural directional cues. J Neurophysiol 70:492–511.

Scheffler K, Bilecen D, Schmid N, Tschopp K, Seelig J (1998): Auditory cortical responses in hearing subjects and unilateral deaf patients as detected by functional magnetic resonance imaging. Cereb Cortex 8:156–163.

Scherg M, Von Cramon D (1986): Evoked dipole source potentials of the human auditory cortex. Electroencephalogr Clin Neurophysiol 65:344–360.

Schönwiesner M, Krumbholz K, Rübsamen R, Fink GR, von Cramon DY (2007): Hemispheric asymmetry for auditory processing in the human auditory brain stem, thalamus, and cortex. Cereb Cortex 17:492–499.

Semple MN, Aitkin LM (1979): Representation of sound frequency and laterality by units in central nucleus of cat inferior colliculus. J Neurophysiol 42:1626–1639.

Semple MN, Kitzes LM (1985): Single-unit responses in the inferior colliculus: Different consequences of contralateral and ipsilateral auditory stimulation. J Neurophysiol 53:1467–1482.

Shaw ME, Hämäläinen MS, Gutschalk A (2013): How anatomical asymmetry of human auditory cortex can lead to a rightward bias in auditory evoked fields. Neuroimage 74:22–29.

Sparks R, Geschwind N (1968): Dichotic listening in man after section of neocortical comissures. Cortex 4:3–16.

Steinmann I, Gutschalk A (2011): Potential fMRI correlates of 40-Hz phase locking in primary auditory cortex, thalamus and midbrain. Neuroimage 54:495–504.

Steinmann I, Gutschalk A (2012): Sustained BOLD and theta activity in auditory cortex are related to slow stimulus fluctuations rather than to pitch. J Neurophysiol 107:3458–3467.

Suzuki M, Kitano H, Kitanishi T, Itou R, Shiino A, Nishida Y, Yazawa Y, Ogawa F, Kitajima K (2002): Cortical and subcortical activation with monaural monosyllabic stimulation by functional MRI. Hear Res 163:37–45.

Tovar-Moll F, Monteiro M, Andrade J, Bramati IE, Vianna-Barbosa R, Marins T, Rodrigues E, Dantas N, Behrens TE, de Oliveira-Souza R (2014): Structural and functional brain rewiring clarifies preserved interhemispheric transfer in humans born without the corpus callosum. Proc Natl Acad Sci USA 111:7843–7848.

Wang Y, Ding N, Ahmar N, Xiang J, Poeppel D, Simon JZ (2012): Sensitivity to temporal modulation rate and spectral bandwidth in the human auditory system: MEG evidence. J Neurophysiol 107:2033–2041.

Westerhausen R, Hugdahl K (2008): The corpus callosum in dichotic listening studies of hemispheric asymmetry: A review of clinical and experimental evidence. Neurosci Biobehav Rev 32:1044–1054.

Woldorff MG, Tempelmann C, Fell J, Tegeler C, Gaschler-Markefski B, Hinrichs H, Heinz HJ, Scheich H (1999): Lateralized auditory spatial perception and the contralaterality of cortical processing as studied with functional magnetic resonance imaging and magnetoencephalography. Hum Brain Mapp 7:49–66.